

# DC/AC Power Converter for Home Scale Electricity Systems Powered by Renewable Energy

Faizal Arya Samman

University of Hasanuddin at Makassar, Indonesia  
Electrical Engineering Department, Kampus Gowa Jl. Poros  
Malino Km. 20, Borongloe 92172, Bontomarannu, Gowa  
e-mail: faizalas@unhas.ac.id

Arie Azhari

University of Hasanuddin at Makassar, Indonesia  
Electrical Engineering Department

**Abstract**—This paper presents the design of a single phase DC/AC Converter or Inverter for home scale electricity systems powered by renewable energy such as photovoltaic system. The power converter is controlled using a microcontroller. The inverter system is firstly modeled and simulated using SPICE, before we design it. A control software, implementing Sinusoidal Pulse-Width Modulation (SPWM) signal generator, is embedded into the microcontroller. The SPWM signal is implemented with a simple on/off set activation based on a scheduled-time. The time schedule is obtained from simulation. This approach results in a simpler program compared to another approach, where sawtooth and sinusoidal signal are compared to obtain the required SPWM signal. The inverter is tested for different load conditions. Using a few load configuration, the THD varies between 1% to 13% depending on the load types and the resistive values on the loads. The inverter output voltage amplitude is also measured, and it changes due to the load changes. (*Abstract*)

**Keywords**—DC/AC Inverter, Power Electronics, Power Converter, Microcontroller (*key words*)

## I. INTRODUCTION

The improvement of the energy conversion efficiency of the solar cell (photovoltaic) is the main factor for the booming of the home scale photovoltaic systems development powered by the photovoltaic. When solar cell materials can convert more than 50% light energy from the sun into electric energy, then the era of renewable energy will soon find its successful revolution. The peak successful will be reached, when the power conversion efficiency approach the number of 90%. It can be guaranteed that many homes and offices will install a small until medium scale photovoltaic system locally to fulfill their energy needs.

Meanwhile, research in the field of power electronics as the main supporter for power processing will also be important theme. The inventions of special purpose power electronics for renewable energy processing are required. The main reason for these needs is due to ambient characteristic of the renewable energy sources. Sunlight, for example, is only temporally available in any local domain area. This condition is also valid for the wind energy with random or even unpredictable availability. The other characteristic of the renewable energy is that most of the them are DC (Direct Current) energy sources.

This work is supported by Research Grant “Penelitian Unggulan Perguruan Tinggi” from The Indonesian Ministry for Research, Technology and Higher Education. (Grant Contract Number: 3357/UN4.21/PL.09/2016)

Our research is now developing a home scale electric installation providing AC dan DC voltage. We discuss this DC power line, because naturally, renewable energy sources generate DC electric power. Natural industrial development of DC-powered electronic consumer equipments are grown rapidly. LED lamps, for example, are powered principally by DC electric, and are now growing in markets. However, for some reasons, AC power line is still required in the future.

Currently, most of household equipments at homes or offices requires AC (Alternating Current) electric power. In order to convert the DC power from the renewable energy sources into AC power for the equipments, then we need a DC/AC converter or inverter circuit. This kind of circuit is designed and explored in this paper. Fig.1 shows the block diagram of the home scale electric system powered by photovoltaic (solar cell) panel. The home electricity provides not only AC but also DC output voltage. This paper will only discuss and focus on the AC parts, i.e. the AC conversion process from DC power of the battery.

Before, we start the detail discussion, we first overview the inverter classification.

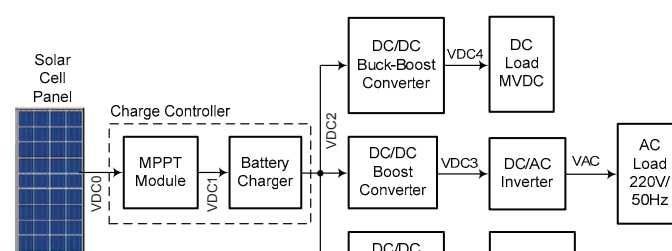


Fig. 1. Home scale photovoltaic system powered by renewable energy.

Inverter can be classified in accordance with its domain of applications, the way its output is controlled, the number of output phases, output voltage handling, and output waveform [1], [2]. According to its phase number, inverter can be classified into three-phase [2], [4] and single-phase inverter [3], [5]. Single-phase inverters can have pure sine waveform [3] or rectangular waveform. The inverters with rectangular output waveform are not recommended for wide applications, since it

generates high total harmonic distortion (THD). The inverter output signals can be handled with transformer or without transformer (transformerless) [6]. The use of transformer is due to the need for higher voltage level, because the DC source is probably lower than the output amplitude requirement. According to its application domain, inverters can be applied on-grid or grid-connected (to power grid utility) and off-grid.

Sinusoidal inverter's output can be achieved with resonant control approach [7], or by using PWM technique [3], [8]. Nowadays, there have been many approaches that can be used to design inverters, from the circuit configuration until control signal algorithms. Power qualities [12], THD and amplitude robustness due to load changes are important issues in the inverter design, beside low cost as well as system and device reliability.

The rest of the paper structure is organized as follows. Section II presents the circuit modeling and simulation of the DC/AC converter circuit using SPICE (Simulation Program with Integrated Circuit Emphasis). SPICE is a industry standard software generally used to simulate analog and digital circuit. This section shows us the transient response and THD (Total Harmonic Distorsion) analysis of the circuit. The software and hardware design step is presented in Section III. Section IV presents the testing results of the realized circuit in hardware. And, then the conclusion and outlooks are presented in Section V.

## II. MODELLING AND SIMULATION

### A. Circuit Modeling using SPICE

The power converter circuit is modeled using SPICE program. The signal generator component is also modeled in the SPICE program. The schematic of the circuits is illustrated in Fig.2. The circuit is designed in full-bridge configuration [2]. We can also design an inverter with half-bridge configuration, however, this approach needs extra control to improve its output quality [5]. Four MOSFET, used as switching devices, i.e.  $M_1$ ,  $M_2$ ,  $M_3$  dan  $M_4$  are respectively driven by four Gate Driver Devices, i.e.  $E_1$ ,  $E_2$ ,  $E_3$  dan  $E_4$ . In general, we can also use insulated-gate bipolar transistors or IGBT [9] as the switching devices. The IGBTs has better operating-voltage level than the MOSFET. However, current MOSFET technology has been improved. MOSFETs based on Silicon Carbide material (SiC MOSFET) have now better power output, including its operating-voltage level, than the conventional MOSFETs [10]. Indeed, MOSFETs developed with Gallium Nitride material (GaN MOSFET) has significant performance (switching speed) improvement than the conventional MOSFET [11].

In the future, SiC-based and GaN-based MOSFETs will be used intensively by industries, due to its better power and switching performance capacity. The unit cost of the devices is unfortunately still high. This paper uses conventional MOSFETs as the switching device. We will improve our design however in the future by using the SiC and GaN MOSFETs.

As shown in Fig.2, a filter is connected to the inverter output port. Hence, loads can be connected in front of the filter.

We use passive filter with LCL configuration. The ECU is used to generate PWM signals, which is then powered-up by Gate Drivers. Gate switching signals conditioned by  $E_1$  and  $E_4$  are similar. Gate drivers  $E_2$  and  $E_3$  also provide similar gate switching signals. In the circuit we give the circuit node numbers, which are used as the reference number for each waveform in the simulation results.

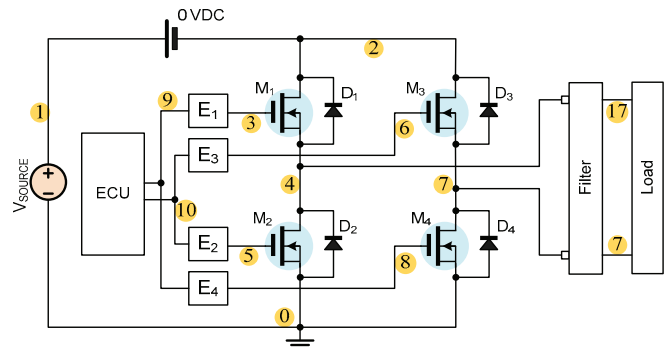


Fig. 2. DC/AC Inverter Circuit Schematics.

### B. Simulation Results

This subsection will show the simulation results of the circuit previously modeled in SPICE code/program. Fig.3 presents the four subplot views. The first line is the sine wave modulator signal and the rectangular signal used to guide the modulation signal. The second line is the absolute of the sine modulator signal and the carrier signal in triangular/sawtooth waveform. Both signals are used to generate PWM control signals for the gate driver as presented in third and fourth line of Fig.3.

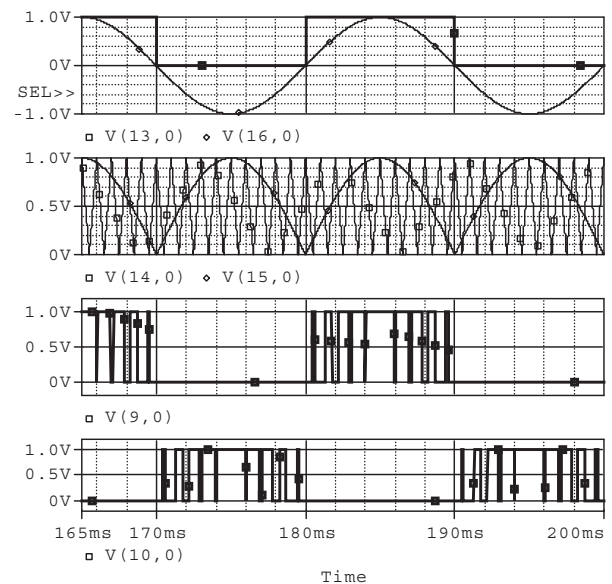
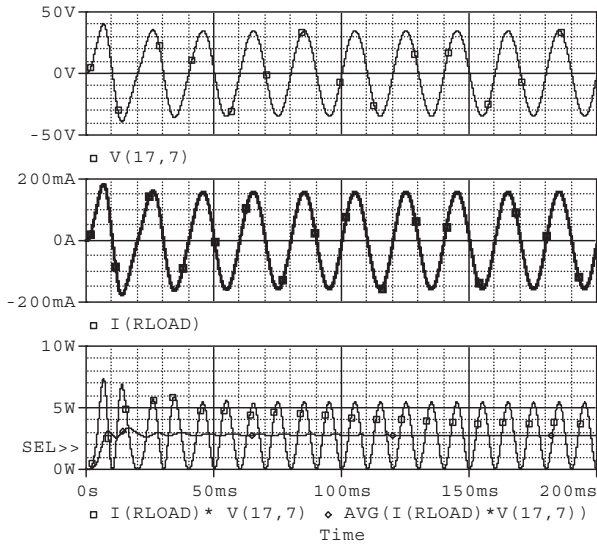


Fig. 3. Modulator, carrier and the generated SPWM signals.

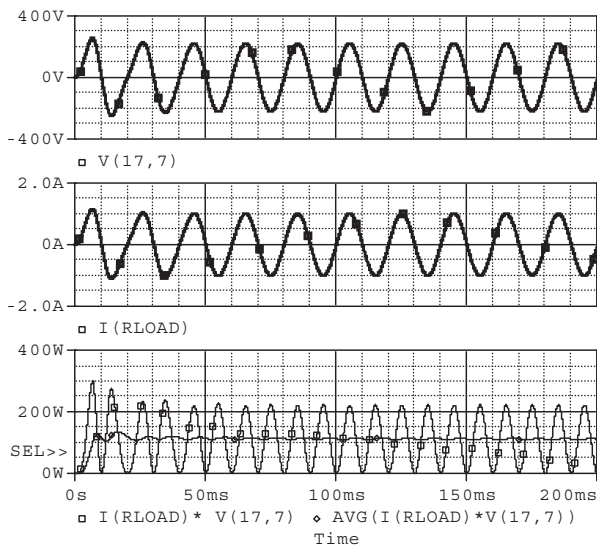
Fig.4 presents the views of three subplot diagram. The first line is the output voltage, the second line is output current and the third line is the power and average power outputs. In this

simulation, a 30V-DC input and 220V-DC input are applied into the input port of the circuit.

Fig.4(a) shows the simulation when we use 30V-DC input, while Fig.4(c) shows is the simulation result when we use 220V-DC input.



(a)



(b)

Fig. 4. Simulation results of the inverter’s output signals with (a) 30V DC input, and (b) 220V DC input.

### III. DESIGN OF THE HARDWARE AND SOFTWARE

There are two main components to realize the DC/AC converter circuit, i.e. hardware and software components. Both are described in the following subsections.

#### A. Hardware and Components

The hardware components are classified into three main parts, i.e. electronic control unit, MOSFET gate drivers and the

power converter circuits. The photography of the hardware is shown in Fig.5.

**Electronic Control Unit:** We use a microcontroller as the main electronic control unit (ECU). A computer program used to generate SPWM signals for the MOSFET’s gate driver is written in C Language.

**MOSFET Gate Drivers:** The gate driver is used to power up the SPWM signals from the microcontroller. Two gate drivers are used. The gate drivers and the microcontroller are isolated each other by an opto-coupler, which is used to protect the low voltage microcontroller from back medium voltage from the power converter circuit. We use TLP250 as the optocoupler devices, and IR2110 as the power gate driver devices.

**Power Converter Circuit:** The DC/AC converter/inverter is designed using full-bridge configuration. The full-bridge structure is shown previously in Fig.2. The realized circuit is shown in Fig.5. We use 4 MOSFETs type IRFP460 as the switching devices. The ECU and power converter circuits are separated for flexibility purpose, i.e. we can use another type of microcontroller or FPGA (Field Programmable Gate Array) in the future.

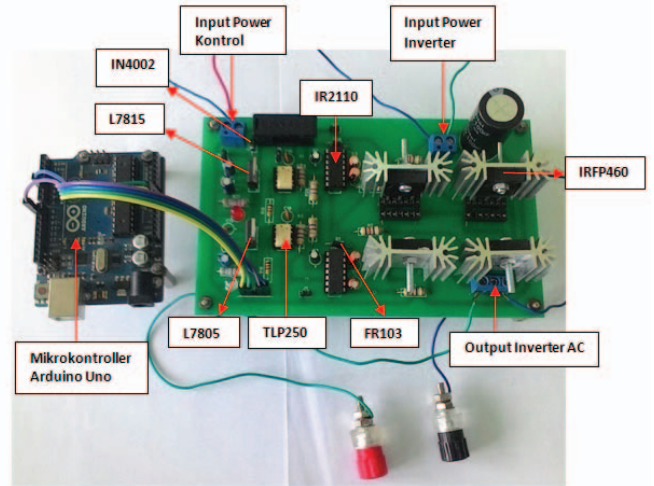


Fig. 5. The Power Converter and its Electronic Control Unit (Microcontroller).

#### B. Embedded Control Software on the Microcontroller

We implement an SPWM signal generator software routine with a simple approach, i.e. on/off set activation for MOSFET gate driving based on a scheduled-time. The time schedule to set and reset the gate signal (SPWM signal) for the MOSFET gates is obtained offline from the simulation. The time schedule is then noted and embedded into the software routine.

This main advantage of the simple approach is to reduce the software complexity while using generally used approach, i.e. comparing the sawtooth signal with the sinusoidal signal to get the required SPWM. The generation of both extra signals will not only increase the control software complexity, but also it can increase control computation latency. Thus, we can get two drawbacks, high power and high delay.



#### IV. TESTING/EXPERIMENTAL RESULTS

This section shows us the testing results of the realized circuit. The testing results are divided into two parts, i.e. general functional test and the test with variable load parameters and configuration.

##### A. General Functional Testing

In this first test, we just measure the functionality of each component in the power electronic circuit. The important test nodes are the inverter output, the SPWM signal generated by the MOSFET's gate power driver. Fig.6 shows the measurement of two SPWM signals using an oscilloscope. As shown in the figure, the SPWM signals are negated each other. Each of them are fed into the gates of two MOSFETs.

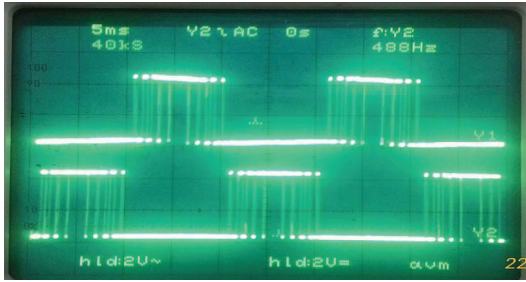


Fig. 6. Measurement of the SPWM signal generated by the power driver.

Fig.7 presents the testing result of the inverter's output voltage without using passive filter. We can see that the waveform of the inverter output voltage is a modulated pulse where its pulse-width is in accordance with the magnitude of the sine modulation signal. When using filter, the sine waveform can be obtained as shown in Fig.8.

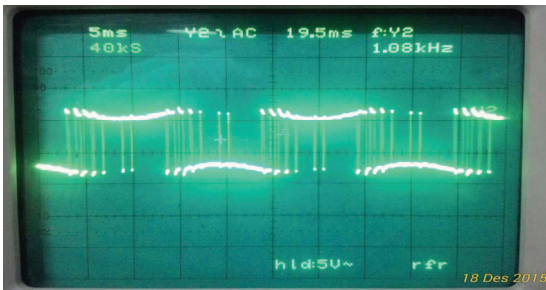


Fig. 7. Testing result of the inverter output before using the filter.

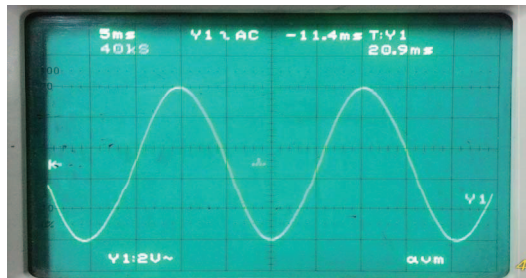


Fig. 8. Testing result of the inverter output after using the filter.

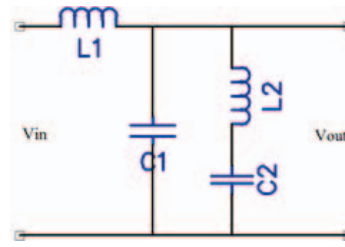


Fig. 9. The passive filter configuration used in the labor experiment.

Fig.9 presents the passive filter configuration used in the experiment. We cannot measure the total harmonic distortion (THD) due to the lack of THD measurement equipment in our Labor. However, we can see that the waveforms are similar to sinusoidal signal. The transfer function of the filter is shown in Eq.(1). We can see that the filter has fourth-order degree.

$$H(s) = \frac{s^2(L_2C_2)+1}{s^4(L_1L_2C_1C_2)+s^2(L_1C_1+L_1C_2+L_2C_2)+1} \quad (1)$$

##### B. Testing with Variable Load

The second test stage is made with variable load parameters and load configurations. There are four load configurations used to test the reliability of the inverter as shown in Fig.10. The first load test is a pure resistive load ( $R_v$ ) as shown in Fig.10(a). The second is a parallel resistive-capacitive load ( $R_v/C$ ) as shown in Fig.10(b). The third is a serial resistive-inductive load ( $R_v+L$ ) as shown in Fig.10(c). The last is resistive-inductive-capacitive load ( $R_v//R+L//C$ ) as shown in Fig.10(d). Certainly, there are many load configurations that can be used to test the inverter performance. However, we are sure that the four load configurations can be good representatives, since they present all kind of possible loads that could be connected to inverters.

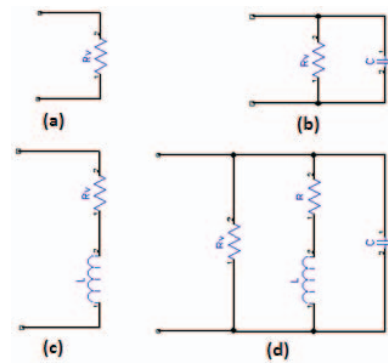


Fig. 10. The passive filter configuration.

The resistive  $R_v$  shown in Fig.10 is a variable resistor. We variate the  $R_v$  value in the experimental tests, and observe the amplitude of the inverter. Table 1 presents the change of amplitude in percent, when the load  $R_v$  is changed for each load configurations. The percentage of in negative value means

that the amplitude of the sinewave voltage is reduced, while the positive percentage means that the amplitude is higher than the DC input voltage. The experiment is done with 30V DC, and the amplitude change percentage ( $A_{CH}$ ) is calculated according to Eq.(2).

$$A_{CH}(\%) = \frac{Amp(V_{OUT}) - V_{DC}}{V_{DC}} \times 100\% \quad (2)$$

From Table 1 we can see that the output voltage amplitude tends to change higher than the input voltage, when the variable resistor  $R_v$  is set to 680  $\Omega$  and 1.5 k $\Omega$  for each load configuration.

Table 1. Change of voltage amplitude for each load configuration.

| Variable Resistor $R_v$ | Change of amplitude of each load configuration |               |                |                     |
|-------------------------|------------------------------------------------|---------------|----------------|---------------------|
|                         | $R_v$ conf.                                    | $R_v+L$ conf. | $R_v//C$ conf. | $R_v//R+L//C$ conf. |
| 220 $\Omega$            | -3.33 %                                        | -3.33 %       | 3.33 %         | -3.33 %             |
| 680 $\Omega$            | 6.67 %                                         | 6.67 %        | 10.00 %        | 6.67 %              |
| 1.5 k $\Omega$          | 13.33 %                                        | 13.33 %       | 16.67 %        | 13.33 %             |

As mentioned early, we cannot unfortunately measure the THD of the inverter output in the labor experiment, since we do not have sufficient equipment to do it. However, in the simulation, we can obtain the measured THD as presented in Fig.11. From the figure, we can see that THD is increased as resistor  $R_v$  is increased for each load configuration. Fig.12 presents the inverter output voltage measurements with different load configuration. Fig.13 presents the inverter output voltages for different values of the variable resistor  $R_v$  using load configuration of  $R_v//R+L//C$ .

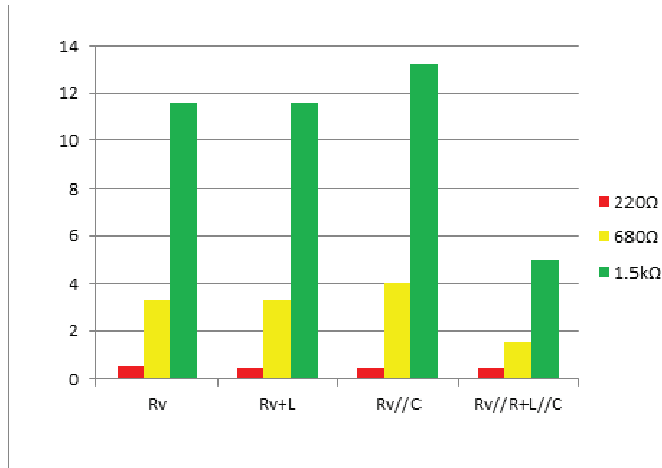
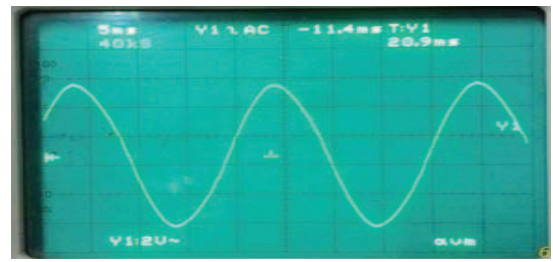
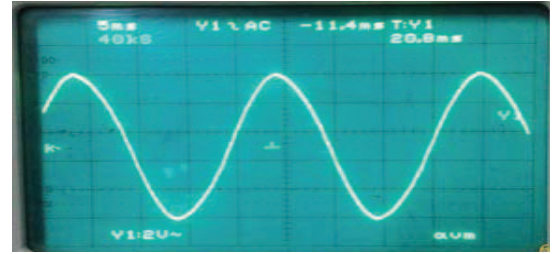


Fig. 11. The THD measurement of the inverter output for four different load configurations and with variable resistive values in the load circuit.

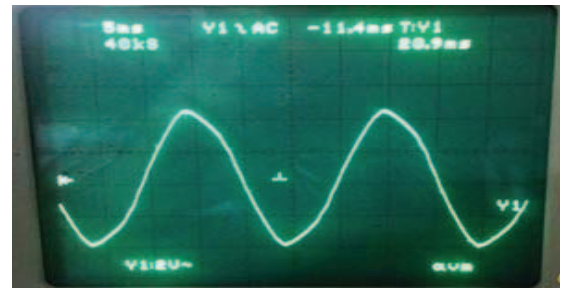


(a)

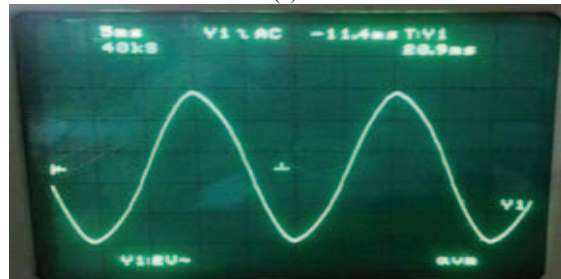


(b)

Fig. 12. Inverter output with load configurations of (a)  $R_v+L$  ( $R_v=1,5$  k $\Omega$ ,  $L=10$  mH), (b)  $R_v//C$  ( $R_v=1,5$  k $\Omega$ ,  $C=3$   $\mu$ F).



(a)



(b)

Fig. 13. Inverter output with load configurations of  $R_v//R+L//C$ , ( $R=1,5$  k $\Omega$ ,  $L=10$  mH,  $C=3$   $\mu$ F) and with variable resistor (a)  $R_v=220$   $\Omega$ , (b)  $R_v=1.5$  k $\Omega$ .

## V. DISCUSSION, CONCLUSIONS AND OUTLOOKS

This paper has presented a DC/AC converter (inverter) for home scale electricity systems powered by photovoltaic electric generation systems. The performance of the inverter over the change of the load parameters and load configurations has been evaluated.

The inverter output voltages are analyzed, as the load configurations are applied to the inverter's output terminal. In simulation stage, the total harmonic distortion (THD) of the inverter is also analyzed. The analysis is done with different load configurations. There are four load configurations used in

the experimental stage, i.e. the pure resistive load, the parallel resistive-capacitive load the serial resistive-inductive load, and the resistive-inductive-capacitive load (Rv//R+L//C). Other load configuration will be used in the future. The experiments are made to observe how reliable the inverter output voltages to response the applied load configuration changes.

The inverter output voltage amplitude will change as load changes with variable configurations connected to the inverter output. The frequency of the inverter output voltages itself does not change as the load changes. Therefore, a mechanism to control these amplitude change, in such a way that inverter's output voltage is maintained at specified amplitude, is required. In future, we will examine this issue by using a specific approach with simple and low power mechanism.

#### ACKNOWLEDGMENT

We would like to thanks the Indonesian Ministry for Research, Technology and Higher Education for the research grant "Penelitian Unggulan Perguruan Tinggi" under Grant Contract Number: 3357/UN4.21/PL.09/2016.

#### REFERENCES

- [1] M. H. Rashid and H. M. Rashid "SPICE for power electronics and electric power, 2nd edition", *CRC, Taylor and Francis*, 2006.
- [2] Faizal A. Samman, Rhiza S. Sadjad, Yasin. "Simulasi dan Analisis Inverter 3-Fasa dengan Sumber Referensi Tegangan pada Jala-jala PLN", *Proc. Seminar Nasional II Rekayasa Material, Sistem manufaktur dan Energi*, 2015, pages:56-62.
- [3] Faizal.A. Samman, Rizkiyanti Ahamd, Mutiah Mustafa. "Perancangan, Simulasi dan Analisis Harmonisa Rangkaian Inverter Satu-Fasa", *Jurnal Nasional Teknik Elektro dan Teknologi Informasi (JNTETI)*, vol. 4, no. 1, Februari 2015, pages 62-70.
- [4] Marcelo G. Villalva, T.G. de Siqueira, M.F. Espindola and E. Ruppert. "Modeling And Control Of A Three-Phase Isolated Grid-Connected Converter For Photovoltaic Applications", *Revista Controle & Automacao*, vol. 22, no.3, May-June 2011, pages: 215-228.
- [5] Yi Zhao; Xin Xiang; Chushan Li; Yunjie Gu; Wuhua Li; Xiangning He, "Single-Phase High Step-up Converter With Improved Multiplier Cell Suitable for Half-Bridge-Based PV Inverter System," *IEEE Transactions on Power Electronics*, vol. 29, no. 6, June 2014, pp. 2807-2816.
- [6] Bin Gu; Jason Dominic; Jih-Sheng Lai; Chien-Liang Chen; Thomas LaBella; Baifeng Chen, "High Reliability and Efficiency Single-Phase Transformerless Inverter for Grid-Connected Photovoltaic Systems", *IEEE Transactions on Power Electronics*, vol. 28, no. 5, May 2013, Pages: 2235-2245.
- [7] Ozdemir S, "Z-source T-type inverter for renewable energy systems with proportional resonant controller", *Elsevier, International Journal of Hydrogen Energy* (2016), dx.doi.org/10.1016/j.ijhydene.2016.01.140. in press.
- [8] C. Bharatiraja S. Jeevananthan, J.L. Munda, and R. Latha. "Improved SVPWM vector selection approaches in OVM region to reduce common-mode voltage for three-level neutral point clamped inverter", *Elsevier, Electrical Power and Energy Systems* vol. 79 (2016) pages: 285-297
- [9] Yanick Lobsiger, and Johann W. Kolar. "Closed-Loop di/dt and dv/dt IGBT Gate Driver", *IEEE Transactions On Power Electronics*, Vol. 30, No. 6, June 2015, pages: 3402-3417.
- [10] Juergen Biela, Mario. Schweizer, Stefan Waffler, and Johann W. Kolar. "SiC versus Si—Evaluation of Potentials for Performance Improvement of Inverter and DC-DC Converter Systems by SiC Power Semiconductors", *IEEE Transactions On Industrial Electronics*, Vol. 58, No. 7, July 2011, pages: 2872-2882.
- [11] Tetsuzo Ueda." GaN, SiC Tout as Next Generation Power Switching Devices", *AEI Magazine, Tech-Focus*, Nov. 2015, pages: 38-41.
- [12] Rashad M. Kamel, "New inverter control for balancing standalone micro-grid phase voltages: A review on MG power quality improvement," *Elsevier, Renewable and Sustainable Energy Reviews*, Vol. 63, Sept. 2016, Pages 520-532.